Amino Acid Residues Controlling Acetylcholinesterase and Butyrylcholinesterase Specificity†

Daniel C. Vellom, Zoran Radić, Ying Li, Natilie A. Pickering, Shelley Camp, and Palmer Taylor*

Department of Pharmacology, University of California, San Diego, La Jolla, California 92093-0636

Received August 5, 1992; Revised Manuscript Received October 23, 1992

ABSTRACT: Acetyl- and butyrylcholinesterase have 51–54% sequence identity in mammalian species; they exhibit distinct substrate and inhibitor specificities. The crystal structure of acetylcholinesterase enables one to predict folding of related esterases as well as assign residues responsible for differences in substrate specificity. These predictions were tested by expression of esterase chimeras and site-specific mutants using mouse acetylcholinesterase as a template. Chimeras of acetylcholinesterase in which the amino-terminal 174 and the carboxyl-terminal 88 amino acids have been converted to the butyrylcholinesterase sequences still exhibit acetyl-like substrate specificity. Four nonconserved amino acids which are within the central sequence and appear to surround the acyl pocket, F_{295}, R_{296}, F_{297}, and V_{300}, have been mutated alone and in combination to the corresponding residues found in butyrylcholinesterase, L_{286}, S_{287}, I_{288}, and G_{291}. The V_{300} and R_{296} mutants slightly enhance butyrylthiocholine hydrolysis while the F_{295} and F_{297} mutants, alone and in combination, confer butyrylcholinesterase character by enhancing activity to butyrylthiocholine, and diminishing activity to acetylthiocholine. The F_{297} mutation eliminates substrate inhibition. F_{295} and F_{297} may form a clamp around the acetoxy methyl group. They have distinctive roles in affecting catalysis of the two acylcholines and precisely control acyl ester specificity. Comparison of the susceptibilities of the chimeras and site-specific mutants to cholinesterase-specific inhibitors isoOMPA, ethopropazine, and BW284c51 suggests that inhibitor selectivity for isoOMPA is attributable to residues limiting the size of the acyl pocket, while residues in the amino-terminal domain presumably near the lip of the gorge affect BW284c51 selectivity. Ethopropazine specificity is governed by residues in the central portion of the sequence but not those in the acyl pocket.

Two types of cholinesterases were distinguished in the 1940's on the basis of distinct substrate specificities in various tissues (Augustinsson, 1948). The acetylcholinesterases (AChE's) exhibit rapid catalysis of acetylcholine hydrolysis, a diminution in rate for propionylcholine, and a marked loss of activity with butyrylcholine. By contrast, the butyrylcholinesterases (BuChE) show far less selectivity for the size of the acyl group and efficiently hydrolyze butyryl- and benzoylcholine. Subsequently, relatively specific inhibitors, BW284c51 for AChE and ethopropazine and isoOMPA for BuChE, enabled investigators to localize AChE and BuChE (Silver, 1974).

The AChE's appear critical to both development and function of the nervous system and the use of AChE inhibitors as therapeutic agents and pesticides has spurred detailed investigations of cholinesterases since their identification by Dale (1914). Although mutations and genetic abnormalities in AChE exist (Bartels et al., 1992), no vertebrates are known to be without the enzyme. BuChE deficiencies are widespread (Whitaker, 1986; Soreq & Zakut, 1990; LaDu et al., 1991). Since the complete absence of BuChE from truncation mutations of the gene does not affect physiologic function in man, BuChE appears nonessential for development and cholinergic neurotransmission. Nevertheless, its appearance in discrete locations during development in the avian nervous system suggests an auxiliary role in developmental processes (Layer, 1991). The population distribution of human BuChE mutations that confer resistance to inhibition by indigenous plant alkaloids points to a role for BuChE in the hydrolysis of certain dietary esters (Soreq & Zakut, 1990). This function is consistent with a prevalence of BuChE in liver and plasma.

While BuChE's have been detected in lower vertebrates (Toutant et al., 1985), analysis of the phylogenetic appearance of the cholinesterases indicates a complex relationship. *Drosophila* has a single cholinesterase whose kinetic properties and sequence relationships lie between those of vertebrate AChE and BuChE (Hall & Spierer, 1986). Recombinant DNA techniques and protein sequencing have revealed that mammalian AChE and BuChE's have 51–54% amino acid identity and complementarity of intrasubunit disulfide linkages (Chatonnet & Lockridge, 1989; Taylor 1991). The recent resolution of a three-dimensional structure of *Torpedo* AChE (Sussman et al., 1991) provides a framework by which related proteins can be modeled. Predictions of structural differences and the functional consequences of individual amino acid or larger domain substitutions can be tested by site-specific mutants and chimeras. Herein, we examine complementarity of domains of AChE and BuChE and assign residues responsible for the substrate and inhibitor specificity of the two esterases from mouse.

MATERIALS AND METHODS

Materials. BW284c51, ethopropazine [10-(2-diethylaminopropyl)phenothiazine], and isoOMPA (tetraisopropylpyrophosphoramide) were products of Sigma Chemical Co., St. Louis, MO. 7-(((Methylethoxy)phosphinyl)oxyl)-1-methylquinolinium (MEPQ) was a gift of Y. Ashani and B. P. Doctor (Levy & Ashani, 1986).

Construction of Chimeras of AChE and BuCHE. Sequences of the previously cloned AChE (hydrophilic form) and

† Supported by USPHS Grant GM18360, USAMRDC Contract No. DAMD17-9-C-1058, and a fellowship to D.V. from the Tobacco-Related Disease Research Program of the University of California, FT43. Z.R. is a visiting Fogarty Fellow from the Institute for Medical Research and Occupational Health, University of Zagreb, Zagreb, Croatia.

* Author to whom correspondence should be addressed.

0006-2960/93/0432-12$04.00/0

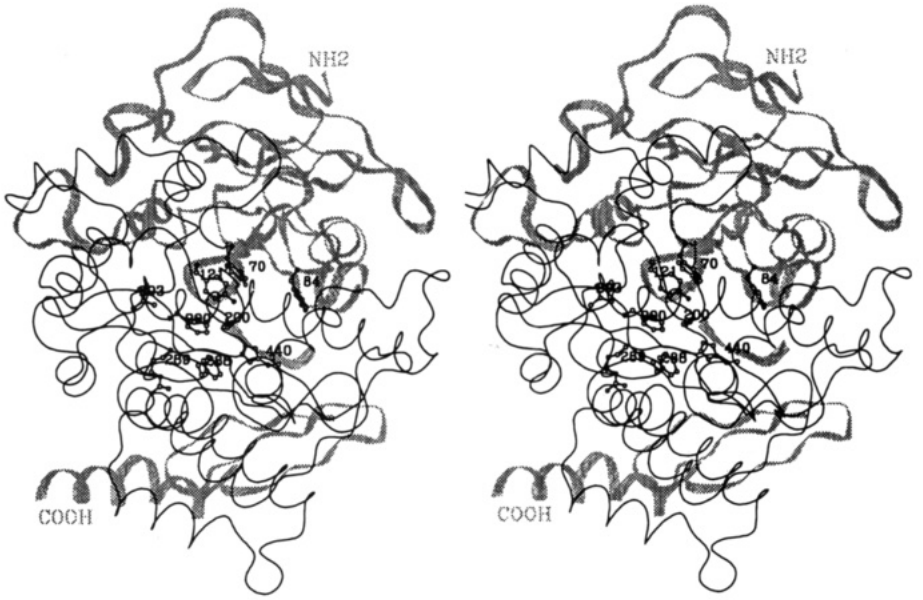

FIGURE 1: Structure of *Torpedo* acetylcholinesterase. The crystal structure is from Sussman et al. (1991). The amino- and carboxyl-terminal domains are displayed as wide ribbons to represent chimeras made by substitution of BuChE sequence. The short, unconnected segment links to the end of the carboxyl-terminal sequence, but the intervening residues are not visible in the crystal structure. Shown are side chain positions of residues mutated in the acyl pocket (F_{288}, R_{289}, F_{290}, V_{293}), catalytic residues (S_{200}, H_{440}), a residue (W_{84}) which stabilizes the choline moiety, and the two aromatic residues within the gorge (Y_{70}, Y_{121}) not conserved in BuChE.

BuChE cDNA's can be found in the EMBO data bank (Rachinsky et al., 1991). An expression construction of BuChE was obtained by linking the 5′ end of the genomic clone to the cDNA at the first coding exon (bp 1033). The insert was cleaved at a *Dra*I site 37 bp 5′ of the initiation methionine and ligated into the expression vector. To construct chimeras of cholinesterase, common restriction sites were generated in both cDNA's. Mutagenic oligonucleotides GGTCTGCTTGATCAACG (bp 607–623) and CGCACAGGTCACCCCAAT (bp 1546–1563) were used to create a mutant AChE gene with *Bcl*I and *Bst*EII sites at positions corresponding to those in the BuChE cDNA. The *Bst*EII site in BuChE was also created with the oligonucleotide CAAAATATGGTCACCCCAAT. To form the chimeras, *Bcl*I to *Bst*EII and *Bcl*I to *Kpn*I (located in the 3′ linker) fragments from the mutated AChE construct were inserted into the BuChE expression vector. Ligation positions were verified by sequencing.

Site-Specific Mutagenesis. Mutant sequences were generated by oligonucleotide-directed substitutions in M13 templates using MutaGene (Bio-Rad) (Kunkel et al., 1987). Mutations were done in an insert bounded by restriction sites *Sph*I at 725 bp and *Pst*I at 1320 bp (Gibney et al., 1990). Silent mutations were also added to generate *Eco*RV and *Xmn*I sites enabling detection of mutants. The insert and its linking regions were sequenced in M-13 by dideoxy sequencing. Wild-type and mutant cDNA's were inserted into a CMV-based expression vector (Andersson et al., 1989). Expression plasmids were purified by two centrifugations on CsCl gradients.

Cell Transfections. HEK-293 cells (American Type Culture Collection) were maintained in Dulbecco's modified Eagle's medium supplemented with 10% fetal calf serum. Cells (10^6/10-cm plate) were transfected 16–24 h after plating with 10 μg of a plasmid DNA–$Ca_3(PO_4)_2$ coprecipitate at pH 7.05 (Gibney et al., 1990). After 24 h, cells were rinsed and placed in serum-free medium. Medium and cells were examined for activity 48–72 h after transfection. Supernatants were concentrated to 1–2% of the original volume by ultrafiltration.

Measurement of AChE Activity and Inhibition: Active Site Titrations. AChE and BuChE activities were measured in 0.1 M $NaPO_4$, pH 7.0, at 22 °C by the assay of Ellman et al. (1961) using acetylthiocholine (ATCh) and butyrylthiocholine (BTCh) as substrates. Active sites were quantitated by titrating with a high-affinity phosphorylating agent, MEPQ, and ascertaining the minimal concentration producing complete inhibition (Levy & Ashani, 1986; Radić et al., 1992). Inhibition by BW284c51 and ethopropazine was measured in the same buffer at four substrate and two inhibitor concentrations in which competitive and noncompetitive inhibition could be established. Two concentrations of isoOMPA were incubated with the enzymes for specified times to estimate the rate constant of irreversible inhibition. Inhibitor and substrate binding to AChE and BuChE was modeled by an energy minimization docking program (Biosym Technologies, Insight II) on a Silicon Graphics Indigo Elan.

RESULTS AND DISCUSSION

Measurement of Catalytic Parameters. Transient transfections into Cos-7 (Gibney et al., 1990) and HEK-293 cells (Velan et al., 1991) provide enzyme in quantities greater than those achieved from injection of mRNA into oocytes (Neville et al., 1992) but not comparable to bacterial expression or specialized viral infections of insect cells (Radić et al., 1992). Nevertheless, sufficient enzyme can be generated for a thorough kinetic characterization. The expressed enzymes are soluble, with more than 70% appearing in the medium. By transferring the cells to serum-free medium, residual activity from serum is minimized. Transfected HEK cells yield up to 28 pmol/10-cm plate. Ultrafiltration of the medium yields 100–200 nM enzyme for direct titration of active centers by MEPQ. Apparent reactivity of MEPQ remains high for the mutants, as evidenced by a linear concentration dependence approaching complete inhibition. Direct titrations, in contrast to antibody precipitation (Gibney et al., 1990), should minimize errors from possible antibody detection of incompletely folded and catalytically inactive protein.

Complementarity of AChE and BuChE Structure: Chimera Kinetics. Torpedo and mouse AChE show 61% residue

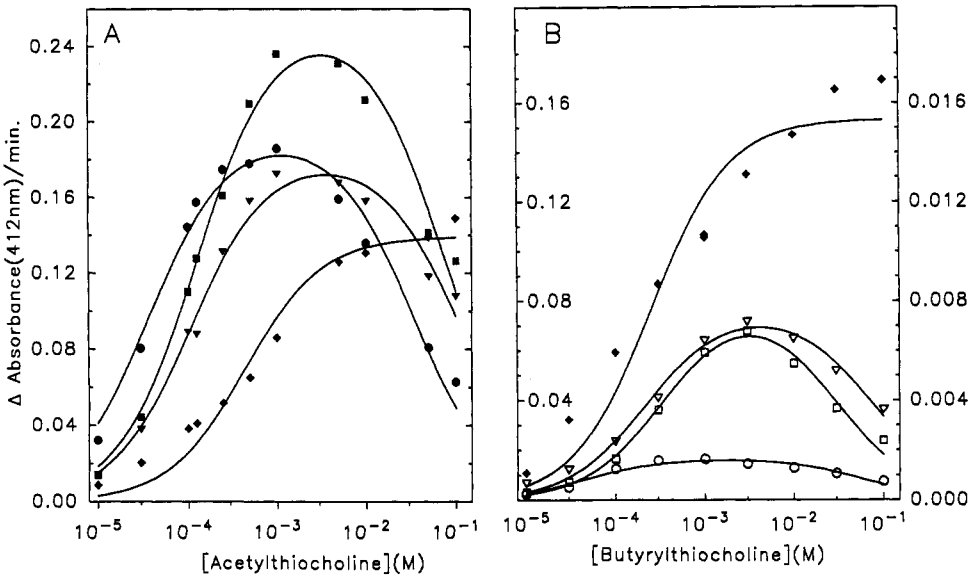

FIGURE 2: Substrate concentration dependences for recombinant mouse AChE (●), mouse BuChE (◆), the B_{5-174}, $A_{175-575}$ chimera (■), and the B_{5-174}, $A_{175-487}$, $B_{488-575}$ chimera (▼). (Panel A) ATCh; (panel B) BTCh. Activities have been normalized to k_{cat} from titration of active sites. The 10× change in scale on the ordinate applies to only BTCh hydrolysis by the two chimeras and AChE (open symbols). Data are fit to the equation in Table I. Lines are generated by a computer best fit analysis. A systematic deviation is found for BuChE which may reflect substrate activation (Webb, 1963) (data not shown).

Table I: Kinetic Constants Calculated for Catalysis of Acetylcholine (ATCh) and Butyrylcholine (BTCh) by Recombinant DNA-Derived Cholinesterases ± Standard Error

wild-type chimera and mutant cholinesterases	K_m (μM) (ATCh)	K_{ss} (mM) (ATCh)	k_{cat} (min^{-1})[a] (ATCh)	k_{cat}/K_m (M^{-1} min^{-1}) (ATCh)	K_m (μM)[b] (BTCh)	K_{ss} (mM)[b] (BTCh)	k_{cat} (BTCh)/ k_{cat} (ATCh)	k_{cat}/K_m (M^{-1} min^{-1}) (BTCh)
AChE	39 ± 2	38 ± 4	17 ± 1.3 × 10^4	4.4 × 10^9	49 ± 3	76 ± 15	0.005 ± 0.001	0.17 × 10^8
BuChE	451 ± 6	–	11 ± 0.2 × 10^4	0.24 × 10^9	280 ± 84	–	0.67 ± 0.03	2.6 × 10^8
B_{5-174}, $A_{175-575}$	140 ± 10	76 ± 0.5	22 ± 0.3 × 10^4	1.6 × 10^9	330 ± 16	28 ± 2	0.016 ± 0.005	0.11 × 10^8
B_{5-174}, $A_{175-487}$, $B_{484-575}$	130 ± 20	96 ± 18	16 ± 5.0 × 10^4	1.2 × 10^9	234 ± 20	65 ± 17	0.032 ± 0.004	0.22 × 10^8
$F_{295} \rightarrow$ L	49 ± 4	62 ± 8	4.4 ± 0.7 × 10^4	0.90 × 10^9	9.0 ± 3	90 ± 5	0.27 ± 0.03	13 × 10^8
$R_{296} \rightarrow$ S	42 ± 5	43 ± 14	11 ± 1.0 × 10^4	2.6 × 10^9	57 ± 15	360 ± 26	0.053 ± 0.003	1.0 × 10^8
$F_{297} \rightarrow$ I	357 ± 66	–	2.7 ± 0.4 × 10^4	0.08 × 10^9	215 ± 12	–	0.34 ± 0.01	0.43 × 10^8
$V_{300} \rightarrow$ G	50 ± 4	46 ± 6	16 ± 2 × 10^4	3.2 × 10^9	100 ± 3	64 ± 3	0.18 ± 0.05	2.9 × 10^8
F_{295}, $F_{297} \rightarrow$ L, I	150 ± 30	355 ± 75	2.0 ± 0.2 × 10^4	0.13 × 10^9	125 ± 5	–	0.58 ± 0.03	0.93 × 10^8
F_{295}, R_{296}, $F_{297} \rightarrow$ L, S, I	138 ± 62	–	1.0 ± 0.5 × 10^4	0.07 × 10^9	ND	ND	0.44 ± 0.07	ND

[a] k_{cat} was determined from at least three titrations of the inhibition of enzyme activity with MEPQ; measurements represent means and standard errors of 3–4 separate transfections. [b] K_m and K_{ss} were calculated from a computer-generated best fit analysis of data similar to Figures 2 and 3 according to the formula: $v = v_{max}/[1 + (K_m/[S]) + ([S]/K_{ss})]$. The fit employed Sigma Plot and was based on a Marquardt least-squares analysis. Values represent means and standard errors from 2–4 separate transfections. [c] A dash indicates substrate inhibition was not detected; ND, not determined.

identity while mouse AChE and BuChE have 53% identity. An interesting feature of the *Torpedo* AChE structure is minimal interdigitation of the amino- and carboxyl-terminal domains which should facilitate formation of cholinesterase chimeras.

Restriction sites were added with silent mutations to enable exchange of BuChE for AChE gene sequences encoding the amino terminus (residues 5–174) and the carboxyl terminus (residues 488–575) (Figure 1). Figure 2 shows the substrate concentration dependencies, and Tables I and II tabulate the catalytic parameters and inhibitor specificities for the chimeras. Little deviation from the properties of recombinant mouse AChE is evident; k_{cat} for ATCh and BTCh are marginally affected, although K_m for ATCh increases slightly. Substrate inhibition is retained in the chimeras, and catalysis for ATCh hydrolysis greatly exceeds that for BTCh. The BuChE selective inhibitors, isoOMPA and ethopropazine (Table II), show minimal increases in inhibitory capacities when BuChE sequences are substituted at the carboxyl- and amino-terminal ends of the molecule. These inhibitors are at least 1000 times more potent on BuChE. These findings are indicative of the overall complementarity of the AChE and BuChE structures. Moreover, the central portion (residues 175–487) of the cholinesterase sequence is responsible for substrate specificity, isoOMPA and ethopropazine inhibitor selectivity, and substrate inhibition. By contrast, the inhibitory capacity of BW284c51 is reduced substantially in both chimeras, suggesting that the amino-terminal domain is largely responsible for its specificity.

Site-Specific Mutagenesis. X-ray structural analysis points to $W_{86(84)}$[1] and $F_{337(330)}$ as residues critical for stabilization of the choline head group and to amide backbone hydrogens at $G_{120(118)}$, $G_{121(119)}$, and $A_{204(201)}$ as forming the oxyanion hole which would hydrogen bond with the carbonyl oxygen (Sussman et al., 1991). The hydroxyl group of $S_{203(200)}$ should be positioned toward the carbonyl carbon. We have used these assumptions for initial placement of the substrate for energy minimization. With this substrate orientation, the acetoxy methyl group would be expected to be configured toward residues 295–297(288–290). Since the latter residues differ in BuChE (Table III), they have been modified singly and in combination. A neighboring residue, $V_{300(293)}$, in AChE

[1] Numbers that follow in parentheses denote the Torpedo numbering.

Table II: Inhibition Constants for the Cholinesterase Chimeras and Site-Directed Mutant Enzymes[a]

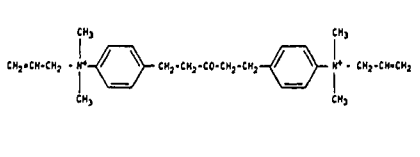

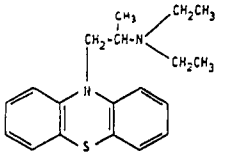

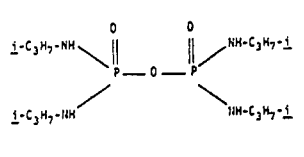

chimera/mutant	K_I (BW284c51) (nM) K_I competitive	αK_I	K_I (ethopropazine) (μM) K_I competitive	αK_I	k_i (isoOMPA) (M^{-1} min^{-1})
AChE		6.5 ± 0.9	≥100		15.9 ± 1.3
BuChE	11300 ± 430	42300 ± 5000	0.062 ± 0.011	0.17 ± 0.03	217000 ± 33000
B_{5-174}, $A_{175-575}$	290 ± 80	1600 ± 200	25	50	51 ± 3
B_{5-174}, $A_{175-487}$, $B_{488-575}$	707 ± 12	1960 ± 50	43	89	108 ± 15
$F_{295} \rightarrow L$		3.1 ± 1.2	≥100		1440 ± 60
$R_{296} \rightarrow S$		1.1 ± 1.0	≥100		142 ± 6
$F_{297} \rightarrow I$		20 ± 17	44	174	3300 ± 400
$V_{300} \rightarrow G$		2.2 ± 0.5	≥100		180 ± 11
F_{295}, $F_{297} \rightarrow$ L, I		19 ± 2	30	111	8500 ± 1250

[a] Inhibition by the reversible inhibitors BW284c51 and ethopropazine was analyzed by construction of reciprocal plots of activity versus substrate concentration. Replots of the slopes and intercepts versus inhibitor concentration yield mixed inhibition from which K_I (competitive) and αK_I are calculated. For ethopropazine, the competitive component is dominant. Standard deviations are derived from the computer-generated replots. No attempt was made to analyze mode of inhibition when K_I exceeded 100 μM. For BW284c51, replots of the slopes for the mutants inhibited at low concentrations do not show linearity, so we did not distinguish the mode of inhibition. k_i for the irreversible inhibitor, isoOMPA, was determined by measuring the rates of inhibition at two isoOMPA concentrations. k_i is directly proportional to inhibitor potency.

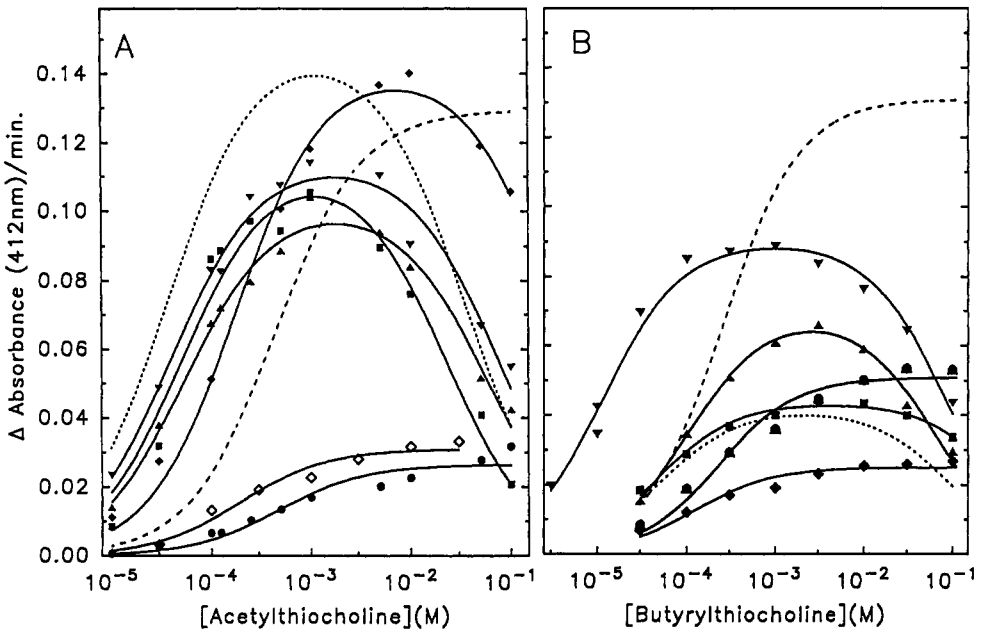

FIGURE 3: Substrate concentration dependencies for site-directed mutants of recombinant mouse cholinesterase. (Dotted line) recombinant AChE; (dashed line) recombinant BuChE. AChE mutants: (▲) $V_{300} \rightarrow G$; (▼) $F_{295} \rightarrow L$; (■) $R_{296} \rightarrow S$; (●) $F_{297} \rightarrow I$; (◆) F_{295}, $F_{297} \rightarrow L$, I; (◇) F_{295}, R_{296}, $F_{297} \rightarrow L$, S, I. (Panel A) ATCh; (panel B) BTCh. Activities have not been normalized to their respective k_{cat} values in order to display a separation of the curves. Data were fit to the equation in Table I. Lines were generated by a computer best fit analysis.

was mutated to G as found in BuChE. The valine side chain might present a steric constraint at the base of the active center gorge. Modification of V_{300} to G, despite being the largest change in side chain volume, did not influence catalytic parameters for ATCh (Figure 3). A similar lack of influence on catalysis is seen with modification of R_{296} to S. The crystal structure shows this arginine side chain pointing away from the active center and stabilized through interactions with $H_{(398)}$ and $N_{(399)}$ in the *Torpedo* enzyme (Figure 4). These mutations affect the K_m slightly and increase k_{cat} for BTCh as anticipated if the steric constraints are diminished.

Modifications of the two phenylalanines, $F_{295} \rightarrow L$ and $F_{297} \rightarrow I$, result in substantial reductions in k_{cat} for ATCh. For the F_{297} mutant, K_m is increased and substrate inhibition is eliminated. The larger K_m and absence of substrate inhibition are characteristic of BuChE. Catalytic efficiency is reduced 50-fold, as measured by k_{cat}/K_m, making this enzyme less efficient for ATCh than the recombinant BuChE. Surprisingly, mutation of F_{295}, but not F_{297}, greatly reduces K_m for BTCh, yielding a value considerably smaller than that for either AChE or BuChE. Both the F_{295} and F_{297} mutations show enhanced k_{cat} values for BTCh. Moreover, F_{295} has a catalytic efficiency for BTCh (k_{cat}/K_m) that exceeds k_{cat}/K_m for BuChE. Simultaneous mutation of the phenylalanines, F_{295} and F_{297}, to the residues in BuChE shows properties similar to the F_{297} mutation. Simultaneous mutation of F_{295}, R_{296}, and F_{297} further reduces catalytic efficiency to where its turnover is ~0.5% of the native enzyme.

Also, F_{297} is critical to substrate inhibition, which is thought to arise from binding of a second substrate molecule to a lower affinity site peripheral to the active center (Radić et al., 1991). Occupation of the peripheral site influences catalytic

Table III: Amino Acid Residues Surrounding the Putative Acyl Pocket in Cholinesterase and Site-Directed Mutants[a]

mouse AChE	F^{295} R F S F V^{300}
human AChE	F^{295} R F S F V^{300}
fetal bovine AChE	F^{295} R F S F V^{300}
Torpedo AChE	F^{288} R F S F V^{293}
Drosophila cholinesterase	F^{329} P – S – A^{332}
mouse BuChE	L^{286} S I N F G^{291}
human BuChE	L^{286} S V N F G^{291}
rabbit BuChE	L^{286} S V N F G^{291}

Site-Directed Mutants residue(s)			
mouse AChE	*Torpedo* AChE	mouse BuChE	mutation
295	(288)	286	F → L
296	(289)	287	R → S
297	(290)	288	F → I
300	(293)	291	V → G
295, 297	(288, 290)	286, 288	F, F → L, I
295, 296, 297	(288, 289, 290)	286, 287, 288	F, R, F → L, S, I

[a] Numbers refer to residues in the mature protein.

efficiency allosterically by altering the orientation of bound substrate or the alignment of residues involved in acylation or deacylation. Previous studies have shown that mutation of $E_{(199)}$ to D in *Torpedo* also eliminates substrate inhibition (Radić et al., 1992). Moreover, it is likely that substrate inhibition can be influenced by changing the conformation of aromatic residues near the lip of the gorge, the probable location of the peripheral anionic site.

Since the putative conformational change associated with substrate inhibition is mediated through the protein, increasing the degree of freedom for substrate binding might be expected to relax the requirements for substrate inhibition. F_{297}, which is absent in BuChE, not only plays a role in orienting substrate to maximize catalysis but also plays one in which its conformation is apparently affected by binding of a second substrate molecule.

The Influence of the Mutations on Inhibitor Specificity. The increase in the BuChE-like specificity for certain mutant AChE's is also evident from an increased rate of isoOMPA inhibition (Table II). IsoOMPA, by phosphorylating the active center serine, is effectively a hemisubstrate in which only the acylation step is rapid. The reaction requires a precise orientation of isoOMPA within the active center, which should resemble the projected tetrahedral geometry of the transition state for carboxyl ester hydrolysis. Selectivity should primarily depend on the dimensions of the acyl pocket, and the isopropylamine in this phosphoramide is closer in dimensions to the butyryl than the acetyl ester. Mutations of one or both of the phenylalanines has the most dramatic effects on isoOMPA reactivity.

Ethopropazine inhibition, by contrast, appears only slightly affected by modification of the acyl pocket with residues found in BuChE. Moreover, the chimeras are not inhibited nearly as well as BuChE. Accordingly, ethopropazine association is minimally affected by the geometry of the acyl pocket or by the residues exchanged by virtue of chimera formation. Selectivity of ethopropazine is likely dictated by domains containing residues between 175 and 487, but not residues 295–300. The binding of ethopropazine may rely primarily on formation of π–π bonds between its phenothiazine ring and $W_{86(84)}$ and $F_{337(330)}$. The latter residue is not conserved in BuChE. The analysis will have to await studies of new mutants or X-ray analysis of its complex with BuChE.

BW284c51, as a long slender molecule, is likely to orient its long axis along the wall of the gorge, one quaternary end

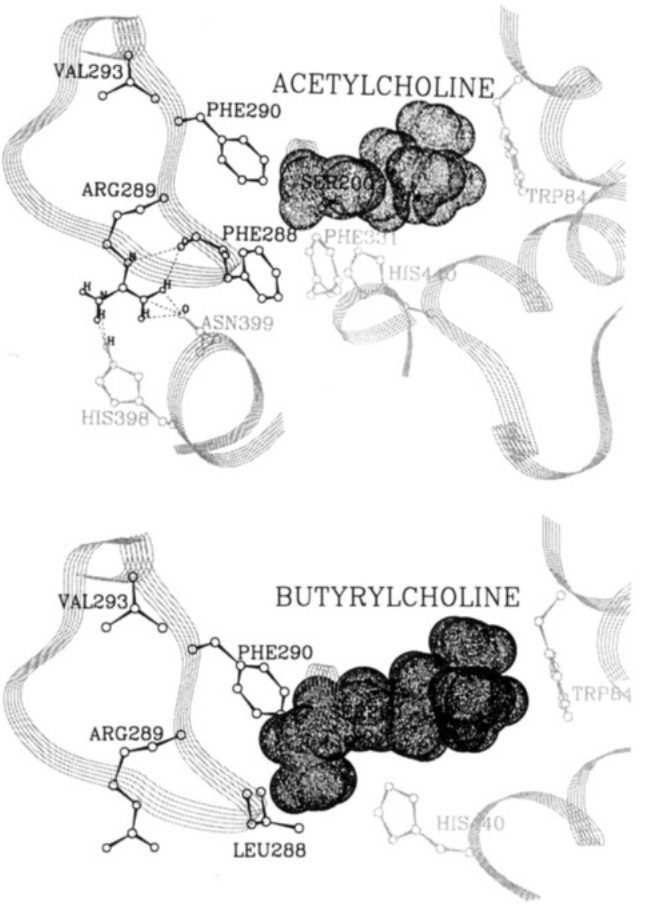

FIGURE 4: Ribbon diagrams of the AChE structure and substrate docked by energy minimization techniques, as described in the test. (Top) Acetylcholine docked to *Torpedo* AChE; (bottom) Butyrylcholine docked to the F_{288} → L mutant of *Torpedo* AChE. Side chains subject to mutation are shown in bold type; other landmark side chains are in light type. Hydrogen bonds are shown by the dotted lines.

being stabilized by W_{86} and F_{337} and the other extending toward the outer rim. Its inhibitory capacity is not affected by modification of the acyl pocket, suggesting an absence of interaction with this region (Table II). However, substitutions in the first 174 residues markedly diminish its inhibition capacity and change the mode of inhibition. Analysis of the mouse AChE structure shows that six of the 15 residues that line the active center gorge in the *Torpedo* AChE X-ray structure are not conserved in mouse BuChE. These residues include $Y_{72(70)}$, $Y_{123(121)}$, $W_{286(279)}$, $F_{295(288)}$, $F_{297(290)}$, and $F_{338(331)}$. Of these, only Y_{72} and Y_{123} exist in the first 174 residues; they likely contribute to stabilization of BW284c51. Docking and energy minimization calculations of the complex show that one end of BW284c51 lies in close apposition to these tyrosines which, in turn, are spatially close to one another (data not shown). Since the chimeric enzymes show normal substrate inhibition, these residues do not form the substrate inhibition site or participate in the conformational changes associated with this phenomenon.

Description of the Acyl Pocket. Analysis of three-dimensional structure of unligated AChE and the mutagenesis studies reported here define the location of the acyl pocket and show that the F_{295} and F_{297} side chains which orient toward the gorge dictate acyl pocket specificity. The intervening arginine side chain is oriented away from the gorge (Sussman et al., 1991) and may anchor this loop by a charge interaction with residues deep within the molecule (Figure 4). The role of the phenylalanines in steric occlusion upon binding of large

acyl chains is obvious, but they may also play a critical role in stabilizing the substrate in an optimal position for catalysis. Hence, the two phenylalanines may outline or form a clamp around the methyl moiety of acetylcholine restricting its degrees of freedom. Substitution of one or both of these side chains with aliphatic residues diminishes the catalytic efficiency of ATCh hydrolysis with the effect on residue 297 being the most dramatic. The efficiency of BTCh hydrolysis is enhanced greatly by elimination of only one phenylalanine, and, curiously, the 295 residue is most critical. In fact, the mutant enzyme appears 5 times more efficient in hydrolyzing BTCh than native BuChE. Substitution of a single phenylalanine may enlarge pocket dimensions sufficiently to preclude steric hindrance for BTCh; simultaneously, the second phenylalanine confers sufficient rigidity to restrict the degrees of freedom of bound BTCh. This offers an explanation for the enhanced efficiency of catalysis of the butyryl ester. Importantly, this finding suggests that acyl ester specificity can be tuned with considerable fidelity by modification of the phenylalanines and adjacent residues. In this regard, Fournier and colleagues (1992) have found a naturally occurring mutation in *Drosophila* cholinesterase in which a phenylalanine corresponding to the 288–290 region in *Torpedo* (Table III) is mutated to tyrosine. This change appears sufficient to diminish the susceptibility of the enzyme to certain organophosphates. Presumably, the added hydroxyl group further constrains the size of the acyl pocket.

ADDED IN PROOF

After this paper was accepted for publication, an article was published (Harel et al., 1992) which describes substrate kinetics and isoOMPA inhibition for one of the above mutants of *Torpedo* AChE, $F_{(288)}F_{(290)}$. The findings are qualitatively similar to those reported here.

REFERENCES

Andersson, S., Davis, D. L., Dahlbäck, H., Jornvall, H., & Russell, D. W. (1989) *J. Biol. Chem. 264*, 8222–8229.

Augustinsson, K. B. (1948) *Acta Physiol. Scand., Suppl. 52*, 1–182.

Bartels, C. F., Zelinski, T., & Lockridge, O. (1992) in *Multidisciplinary Approaches to Cholinesterase Function* (Shafferman, A., & Velan, B., Eds.) Plenum Press, London.

Chatonnet, A., & Lockridge, O. (1989) *Biochem. J. 260*, 625–634.

Dale, H. H. (1914) *J. Pharmacol. Exp. Ther. 6*, 147–190.

Ellman, G. C., Courtney, K. D., Andres, V., Jr., & Featherstone, R. M. (1961) *Biochem. Pharmacol. 7*, 88–95.

Fournier, D., Bride, J. M., Hoffman, F., & Karch, F. (1992) *J. Biol. Chem. 267*, 14270–14274.

Gibney, G., Camp, S., Dionne, M., MacPhee-Quigley, K., & Taylor, P. (1990) *Proc. Natl. Acad. Sci. U.S.A. 87*, 7546–7550.

Hall, L. M. C., & Spierer, P. (1986) *EMBO J. 5*, 2949–2954.

Harel, M., Sussman, J. L., Krejci, E., Bon, S., Chanal, P., Massoulié, J., & Silman, I. (1992) *Proc. Natl. Acad Sci U.S.A. 89*, 10827–10831.

Kunkel, T. A., Roberts, J. D., & Zakour, B. A. (1987) *Methods Enzymol. 154*, 367–382.

LaDu, B. N., Bartels, C. F., Nogueira, C. P., Arpagaus, M., & Lockridge, O. (1991) *Cell. Mol. Neurobiol. 11*, 79–89.

Layer, P. G. (1991) *Cell. Mol. Neurobiol. 11*, 7–33.

Levy, D., & Ashani, Y. (1986) *Biochem. Pharmacol. 35*, 1079–1085.

Neville, L. F., Gnatt, A., Loewenstein, Y., Seidman, S., Ehrlich, G., & Soreq, H. (1992) *EMBO J. 11*, 1641–1649.

Rachinsky, T. L., Camp, S., Li, Y., Ekström, T. J., Newton, M., & Taylor, P. (1990) *Neuron 5*, 317–327.

Radić, Z., Reiner, E., & Taylor, P. (1991) *Mol. Pharmacol. 39*, 98–104.

Radić, Z., Gibney, G., Kawamato, S., Bongiorno, C., & Taylor, P. (1992) *Biochemistry 31*, 9760–9767.

Silver, A. (1974) *The Biology of the Cholinesterases*, North Holland, Amsterdam.

Soreq, H., & Zakut, H. (1990) *Cholinesterase Genes: Multileveled Regulation Monographs in Human Genetics* (Sparkes, R. S., Ed.) Karger, Basel.

Sussman, J. L., Harel, M., Frolow, F., Oefner, C., Goldman, A., Token, L., & Silman, I. (1991) *Science 253*, 872-878.

Taylor, P. (1991) *J. Biol. Chem. 266*, 4025–4028.

Toutant, J. P., Massoulie, J., & Bon, S. (1985) *J. Neurochem. 44*, 580–592.

Velan, B., Grosfeld, H., Kronman, C., Leitner, M., Gozes, Y., Lazar, F., Flashner, Y., Cohen, S., & Shafferman, A. (1991) *J. Biol. Chem. 266*, 23977–23984.

Webb, J. L. (1963) *Enzyme & Metabolic Inhibitors*, pp 46–47, Vol. 1, Academic Press, New York.

Whitaker, M. (1986) in *Cholinesterases: Monographs in Human Genetics* (Beckman, L., Ed.) Vol. 11, Karger, Basel.